OPTICAL EMISSION SPECTRUM OF THE UK-10 ION THRUSTER OPERATING ON XENON

88-112

P. M. Latham, A. R. Martin and M. T. Cresdee
Culham Laboratory, Abingdon, Oxon OX14 3DB, England

Abstract

This paper describes measurements of the optical emission spectrum of the UK-10 thruster operating with a xenon propellant. Measurements of relative intensity were made as a function of wavelength in the range 350-850 nm. Two fields of view were investigated, one looking towards the beam a little downstream of the extraction grids, the other looking directly at the grids into the discharge chamber. The data obtained have been compared with similar published optical measurements on mercury thrusters, and the implications for integration with spacecraft and some specific scientific instruments have been re-considered. No problems are anticipated from this point of view.

1. INTRODUCTION

Ion thruster systems presently under consideration for a range of station-keeping, orbit raising, and deep space missions necessarily interact with both the spacecraft and the surrounding space plasma. A proper assessment of the effects of these interactions is essential to gaining full acceptability of electric propulsion systems. A major area of concern is spacecraft contamination from thruster exhaust efflux, but electromagnetic interference from thruster operation, electric and magnetic fields, and optical interference have all been considered. With the increasing preference for using xenon instead of mercury, all these areas are being actively re-assessed.

This paper describes a first examination of the optical emission spectrum of a xenon ion thruster. Previous work on mercury thrusters has shown that optical interference has a minimal effect on almost all instruments considered, particularly when compared with the more serious problems associated with thruster efflux. Nevertheless, the same must be demonstrated to be true for xenon operation. This paper aims to contribute to this effort.

2. EXPERIMENTAL DESCRIPTION

The measurements described here were performed on a T4A 10 cm thruster, which is identical to the T5 flight version as far as all relevant discharge and beam properties are concerned. The thruster was operated in the Culham Laboratory Ion Thruster Test Facility. This facility has a vacuum chamber 5.9 m in length, 1.3 m in diameter, and employs liquid helium cryopumps to pump the large gas loads and maintain a low pressure in the facility during rare gas operation.

The base pressure is below 4×10^{-8} torr and the maximum pumping speed in xenon is 34,000 ls^{-1}. Typical pressures during measurements were around $1\text{-}2 \times 10^{-5}$ torr. Figure 1 is a schematic diagram of the facility, showing the general chamber construction, and the thruster and observation ports positioning. Also shown is the position of the optical equipment and the approximate field of view used in these measurements.

Figure 2 shows the optical system in more detail. All measurements were made using a Rofin Model 6000 monochromator operated with a Rofin Model 6001 wavelength marker. The monochromator used a blazed grating, with a blaze wavelength of 300 nm, which scanned a wavelength range of 300-1100 nm with a scan period of about 95 ms. Light from the thruster beam or grids, passing through the fused silica glass ports was focused onto the monochromator entrance slits in such a way as to maximise the monochromator efficiency. Both entrance and exit slits had a bandpass corresponding to 2 nm. The light dispersed from the grating was fed via the exit slits and a light guide to the detector.

The detector consisted of an EMI type 9658 photomultiplier. This has a relatively high response in the infra-red region, which allowed measurement in the wavelength range from about 350 nm to 850 nm; the spectral response is shown in Figure 3, together with that of a standard, non red enhanced, phototube.

The spectral range covered exceeds 2:1, but no precautions were taken at this stage to avoid second order and re-entrant peaks in the spectra. For the instrument used such peaks would have a typical amplitude of 0.5-2% of the input wavelength peak amplitude, and would not affect the conclusions of this study.

The detector output was displayed on a Nicolet 4094 digital oscilloscope together with the synchronised wavelength calibration signal from the 6001 marker. The Nicolet 4094 allowed digital signal averaging, storage of the time-synchronised detector and wavelength marker signals, and data transfer to computer for further processing. This processing involved correcting for the spectral variation of the quantum efficiency of the 9658 photomultiplier and the diffraction grating efficiency of the monochromator to produce a spectrum directly proportional to the absolute intensity. The numerical fit to the diffraction grating efficiency used to correct the spectrum is shown in Figure 4.

3. EMISSIONS FROM THE BEAM

3.1 Overall Features of the Xenon Spectrum

For beam measurements, the monochromator was positioned to detect light within an angle roughly corresponding from 10 cm to 40 cm downstream of the grids, thus excluding light from the discharge itself, while examining the region giving the highest overall emissive power. It was unfortunately not possible to calibrate the detector with a standard source and thereby obtain absolute intensities. All quoted intensities are, therefore, in arbitrary units.

Figure 5 shows the emission spectrum from the beam, before and after correction, for thruster operation close to its nominal 25 mN. The signal was digitally averaged. Relative intensities of these lines are listed in Table 1, and other strong lines outside the measurement range in Table 2. Both tables are derived from Ref. 1.

The emission spectra of xenon and the other rare gases were among the earliest to be studied by spectroscopists, and much detailed information on emissions from low pressure sources exists. To allow direct comparison with the present measurements, a program was written to display this data in a similar format. The resulting histogram, covering the 130 most intense XeI and XeII lines, is shown in

Figure 6; the intensity data are from Ref. 2. The equivalent histogram for mercury is very useful for demonstrating the comparative simplicity of its spectrum. This is considered in more detail later.

Comparison of Figures 5 and 6 shows that the measured beam spectrum clearly reproduces the features which would be expected from a low pressure optically thin plasma. The series of lines in the range 410-550 nm appears strongly in the beam, with a band of lower intensity lines in the 600-820 nm range, and the very intense near infra-red lines at around 825 nm. This was very close to the wavelength limit for the detector.

There are obviously intensity differences between the measured thruster beam and those predicted from the histogram. In part these will be due to monochromator and photomultiplier variations from published specifications. However, the most likely reason for any intensity mismatch is that correlation of intensities between different sources using different detectors has historically been difficult. Nevertheless, it is concluded that the main features of the beam spectrum may be accurately predicted from published spectroscopic data.

Considering briefly the resolution obtained in Figure 5, this appears to be around 5 nm. This is adequate for present purposes, but could be improved if required. As an example, if fewer averages were performed, accepting poorer signal/noise ratios, resolution was improved. For example, resolution of the two peaks around 825 nm was possible. However, in the context of implications for missions employing electric propulsion systems, this is not critical.

3.2 Intensity Variation with Thruster Operating Parameters

The intensity variation was investigated for two thruster parameters, the beam voltage and beam current. The beam voltage was raised from the nominal 25 mN value of 1,100 V to 1,300 V and then 1,500 V, where the spectra were taken again under otherwise identical conditions. The three (uncorrected) traces are shown in Figures 7, 8 and 9; the profiles are almost identical, apart from the overall intensities which are roughly proportional to the beam voltage. Similarly, holding the beam voltage constant at 1,100 V, the beam current was dropped from its nominal value of 457 mA in Figure 7 to half this value in Figure 10. This reduces the overall intensity by roughly a half (though not the noise), preserving the main features of the profile.

3.3 Comparison with Mercury Data

Goldstein and Monahan[3] performed a range of emission measurements and calculations on a 30 cm engineering model thruster running on mercury. Both spectral and total integrated intensity measurements were made, the photomultiplier chosen being sensitive in the range 160 nm to 600 nm. For spectral measurements, a scanning monochromator was used to disperse the light. Table 3 (derived from Ref. 1) gives the wavelengths found for a typical spectrum taken with a 1 A beam current: the five strongest HgI lines are shown; at higher sensitivity, a 291.5 nm HgII transition was also visible.

The 30 cm thruster could be gimballed to allow beam profile measurements, and the total intensity profiles were measured for different beam voltages and currents. The profiles themselves were parabolic near the core and exponential on the wings, in agreement with current density measurements. The three voltages used were 500 V, 700 V and 1,100 V and the peak intensity was proportional to the beam (screen) voltage. In the present work in xenon the intensity at individual wavelengths was found to be roughly proportional to voltage, though there was some wavelength dependence.

Similarly, the dependence of total and spectral line intensity on beam current was also determined for the five mercury lines. This was found to be proportional to beam current, again in agreement with the present xenon observations.

3.4 Reasons for Differences in the Xenon and Mercury Spectra

The simplicity of the mercury spectrum when compared with that of xenon is striking. This is made clearer in Figure 11 which is an equivalent histogram to that produced earlier for xenon. The same wavelength range is used, and all lines of intensity greater than 2% of the most intense line are included - the same criterion used for the xenon histogram. (The 253.7 nm line seen in second order by Goldstein and Monahan at 507.3 nm has been added). Reasons for the relative complexity of the xenon spectrum may be found by considering the electron configurations and allowed transitions in the various atomic species.

The HgI and HgII ground state electron configurations are $5s^2 5p^6 5d^{10}\ 6s^2$, and $6s^1$ respectively. Normally, a single 6s electron is excited to higher levels. In the L-S (Russell-Saunders) coupling approximation, (where L is the total orbital and S the total spin angular momenta) the residual electrostatic interaction is considered first, with the spin-orbit interaction added as a perturbation. The HgI and HgII ground state terms are $^1S_0$ and $^2S_{½}$ respectively. The L-S coupling approximation is good for the lighter elements in the periodic table, but generally poorer for heavier elements such as mercury. One of the most intense mercury lines results in fact from the forbidden transition of the metastable $6^3P_1 - 6^1S_0$. (Transitions from the $^3P_{0,2}$ terms are strictly forbidden by the selection rules $\Delta J = 0, 1$, but not $J = 0 \rightarrow J = 0$, where $J = L + S$). For HgII, there is only a single optically active electron, and for HgI an extra electron is added to the 6s level with zero orbital angular momentum. The consequences of this are that the spectra produced by these species are fairly simple and the spacing of energy levels leads to the spectra being dominated by just a few lines.

In the case of XeI and XeII, with ground state configurations $5s^2 5p^6$ and $5s^2 5p^5$, electrons are excited out of the inner 5p shell effectively leaving a hole with orbital and spin angular momenta of the missing electron(s).

The energy required to do this is relatively large, and this has a number of consequences, one being strong transition lines in the ultra-violet region of the spectrum. A second consequence, which is common to all the rare gases and related species with one or two electrons missing from a core, is that a $\underline{J}$-$\underline{\ell}$ coupling scheme best describes the observed energy levels. In this scheme, the total angular momentum ($\underline{J}$) of the core (containing a one or two electron hole) couples with the orbital angular momentum ($\underline{\ell}$) of the single electron excited into a much higher level.

The terms resulting from the $\underline{J}$-$\underline{\ell}$ coupling of the core hole and outer electron can be quite complex with far greater possibilities for transitions to the ground state. The large energy difference between core and higher levels also means that many transitions will appear over a comparatively narrow part of the spectrum. Taken together, all these factors help to account for the apparent complexity of the xenon spectrum when compared with that of

mercury.

4. DISCHARGE MEASUREMENTS

The other field-of-view examined was that looking directly at the discharge chamber through the grids, both with and without extracting a beam current. Figures 12, 13 and 14 show the spectra (corrected and uncorrected) for discharge currents of 5.0 A, 2.5 A and 1.0 A respectively; the intensity scales are directly comparable. Though clearly there are variations with wavelength, overall, the intensities vary approximately in proportion to the discharge current. The corrected spectra are again dominated by the strong peaks at around 825 nm. In the case of mercury, the intensity of the 235.7 nm HgI line was found roughly proportional to discharge current for an equivalent field-of-view.

On extracting a beam, in the 5.0 A case, the only significant change was a reduction in intensities by about 20%. Without altering any thruster or spectrometer parameters, the monochromator was then moved back to the beam field-of-view to obtain a value for the intensity ratio. This ratio for discharge-to-beam intensity was (85+/-5):1; the change in monochromator-to-source distance was small but its effect was included in the above value.

5. IMPLICATIONS OF OPTICAL EMISSIONS FOR SPACECRAFT INTEGRATION

5.1 Science Instruments

Possible interference problems from optical emissions were considered by Goldstein and Monahan[3] in the mercury measurements mentioned above. An absolute intensity calibration was made, from which an empirical volume emission rate was derived. Photon production rates were calculated as a function of wavelength, and these were compared with the sensitivities of a range of scientific instruments, specifically chosen to provide an assessment over a wide range of wavelengths.

The effect on an ultra-violet spectrometer placed parallel to the thruster axis was calculated. Despite the strong ultra-violet emissions from the HgI and HgII lines, these were a factor of 10 below the spectrometer's minimum detectable signal. Similarly, a spectroheliograph (sensitive in the soft x-ray/EUV region) was predicted to be unaffected, as were an infra-red spectrometer (range 3.0-40.0 μm) and radiometer (range 0.3-40.0 μm). Only one instrument, a zodiacal photometer which is very sensitive in the optical region of the spectrum, could not be operated with a field-of-view intersecting a thruster plume.

Since it was not possible in these present measurements to obtain an absolute intensity calibration, a similar analysis of specific scientific instruments is difficult. One clear difference in the spectra is the appearance of strong lines in the infra-red, for which allowance must be made.

It is worth noting, as indicated in Table 2, that there are no significant lines expected in the UV in the range from 130-350 mn, and hence the UV spectrum appears relatively clean.

There is a need for absolute intensity calibration, and for spectral investigation in the UV and IR ranges to ensure full compatibility of xenon with science instruments.

5.2 Star Trackers

A particular concern for one early application of the UK-10 system is any interference with the operation of a star tracker. This is, therefore, considered below, applying the results of the xenon measurements.

A modern two-axis star tracker can be thought of as a kind of television camera. A star field is imaged by a suitable lens onto a solid-state imager such as a charge-coupled device (CCD). The position of a star image on the CCD indicates the angle subtended with the optical axis, or "boresight" of the tracker.

In a typical star tracker device, such as that developed by SIRA for the ROSAT x-ray astronomy satellite[4,5], the bandpass of the CCD is optimised for 500-750 nm by the blue cut-offs of the glass used in the optics of the tracker system and the detector, and by an infra-red blocking filter applied to one of the lens surfaces. This reduces the optical design problems, and also reduces the difference in sensitivity to the red and blue stars.

Referring to the xenon optical spectrum, it can be seen that the blue cut-off will probably have to be shifted to 560-570 nm. This limitation of range should not cause a problem, apart from a loss of sensitivity. A faster lens could be used in the optical system to compensate for this. The range could also be shifted further into the red, up to 800-810 nm, by changing the IR blocking filter characteristics.

The presence of a faint continuum, such as that in the range from 560-810 nm should not present a problem, as long as it is relatively uniform (i.e. similar to a DC offset), and as long as it is small in amplitude compared with the dynamic range of the star tracker itself.

It would appear, then, that the operation of star trackers on-board a spacecraft should not be affected by the presence of a xenon beam, as long as a minor adjustment to the nominal spectral bandpass is made. Systems operating in the range from 570-800 nm should function satisfactorily.

6. CONCLUSIONS

The optical emission spectrum of the UK-10 thruster, operating with a xenon propellant, has been measured over a wavelength range of 350-850 nm. The results are in good agreement with published spectroscopic data on xenon and it is, therefore, expected that extrapolation to emissions outside this wavelength range are valid.

The xenon spectrum has been compared with similar published optical measurements on mercury thrusters. The relative complexity of the detailed xenon spectrum has been demonstrated and the reasons for this discussed. The implications for integration with some specific spacecraft scientific instruments have been re-considered, and no problems are anticipated from this point of view.

Table 1
Strong Lines Present in the Xenon Spectrum
300-850 nm

Wavelength (nm)	Relative Intensity	Species
418.0	1,000	XeII
433.0	1,000	XeII
446.2	1,000	XeII
473.4	600	XeI
491.6	500	XeI
492.3	500	XeI
508.0	1,000	XeII
529.2	2,000	XeII
531.4	1,000	XeII
533.9	2,000	XeII
541.9	3,000	XeII
547.2	1,000	XeII
823.2	10,000	XeI
828.0	7,000	XeI

Table 2
Other Xenon Lines Expected but outside instrument detection range

	Wavelength (nm)	Relative Intensity	Species
UV:	104.1	1,100	XeII
	104.8	1,000	XeII
	105.2	1,200	XeII
	107.4	2,000	XeII
	110.0	1,200	XeI
	129.5	1,000	XeI
IR:	881.9	5,000	XeI
	979.9	2,000	XeI
	992.3	3,000	XeI
	1262.3	2,500	XeI
	1365.7	2,000	XeI
	1473.2	3,000	XeI
	1541.8	2,500	XeI
	2026.2	3,000	XeI
	2651.0	2,500	XeI
	3106.9	6,000	XeI
	3366.7	3,500	XeI
	3507.0	5,000	XeI

Table 3
Strong Lines Present in the Mercury Spectrum
160-600 nm

Wavelength (nm) (Ref.3)	Intensity (Ref.1)	Species
253.7	15,000	HgI
365.0	2,800	HgI
404.7	1,800	HgI
435.8	4,000	HgI
*507.4	-	HgI
546.1	1,100	HgI

* Second Order 253.7 nm Line

REFERENCES

1. R. C. Weast (Ed.), CRC Handbook of Chemistry and Physics, 62nd Edition, 1981/82.

2. A. N. Zaidel', V. K. Prokof'ev et al, Tables of Spectral Lines, Plenum Press, 1970.

3. R. Goldstein and K. M. Monahan, Optical Properties of Mercury Ion Thruster Exhaust Plumes: Significance for Candidate SEP Science Instruments, AIAA Paper 75-362, March 1975.

4. G. Lange, B. Mossbacher and D. Purll, The ROSAT Star Tracker, in Instrumentation in Astronomy, D. L. Crawford (Ed), SPIE, 627, 243-253, (1986).

5. G. R. Hopkinson, R. A. Cockshott, D. J. Purll, M. D. Skipper and B. Taylor, Operation, Performance and Reliability Testing of Charge-Coupled Devices for Star Trackers, Opt. Eng., 26, 725-733 (1987).

ACKNOWLEDGEMENT

This work was sponsored and monitored by Space Department, Royal Aerospace Establishment (RAE) Farnborough.

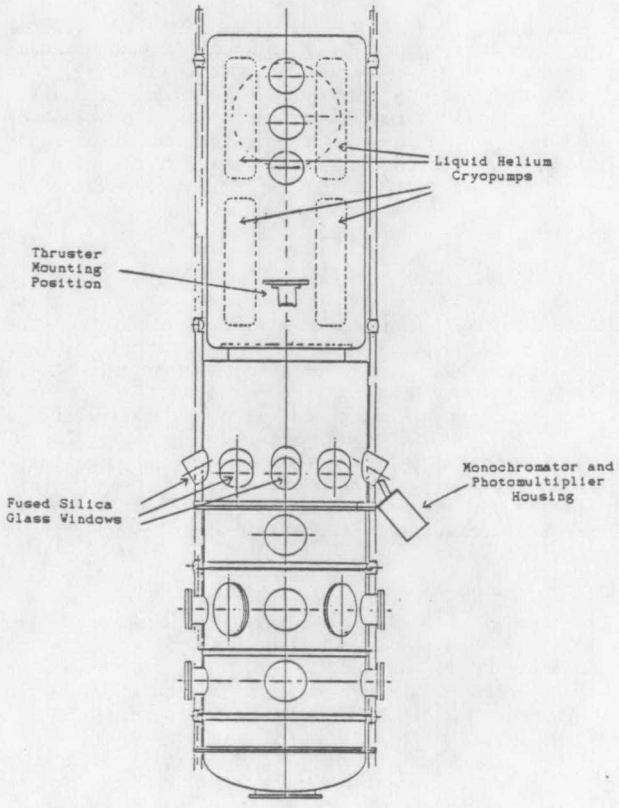

Figure 1. Layout of the Ion Thruster Test Facility

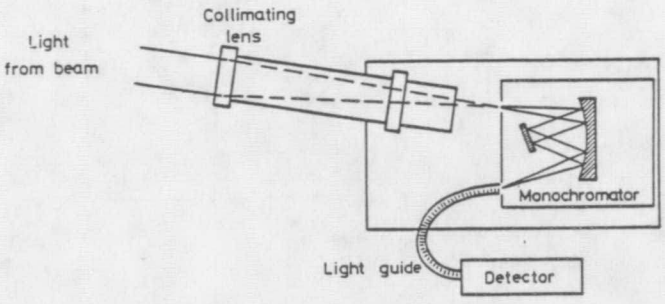

Figure 2. Detail of the Optical Measurement System

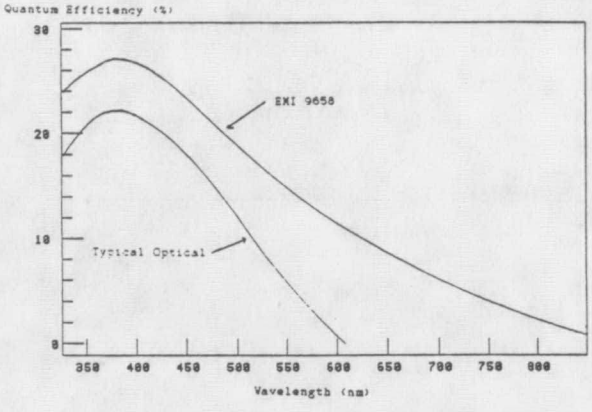

Figure 3. Spectral Responses of the EMI 9658 Photomultiplier and a typical non red enhanced phototube

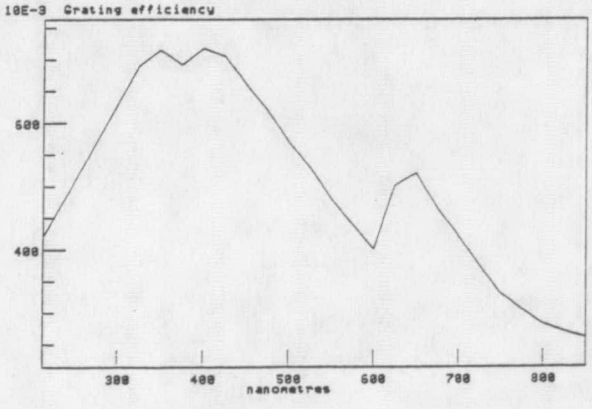

Figure 4. Diffraction grating efficiency used for processing spectra.

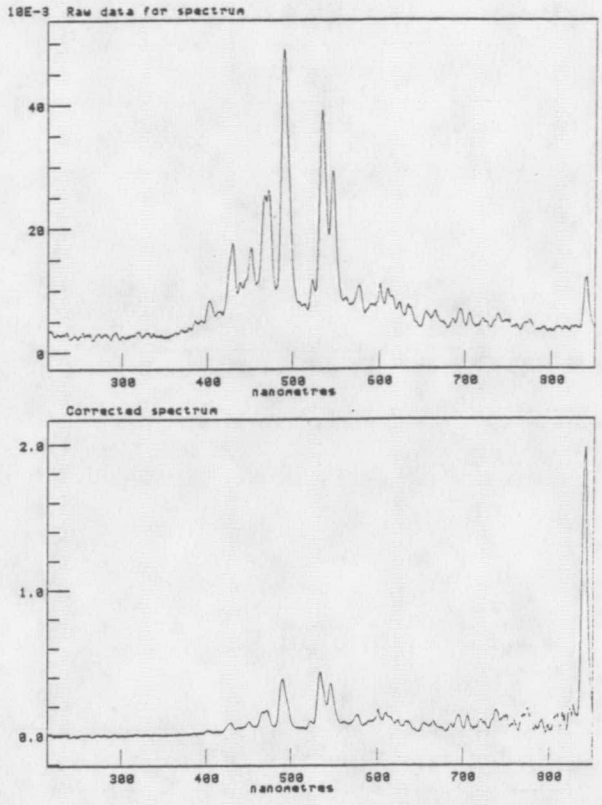

Figure 5. Uncorrected and Corrected Beam Spectrum

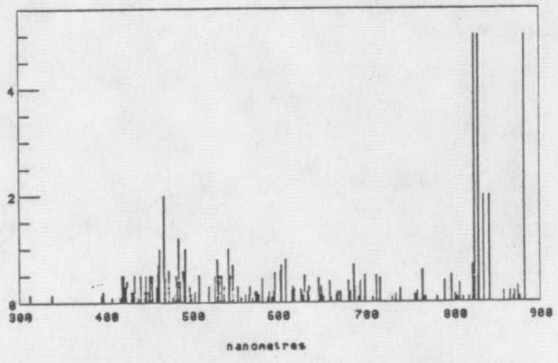

Figure 6. Computer Generated Histogram of the Xenon Spectrum

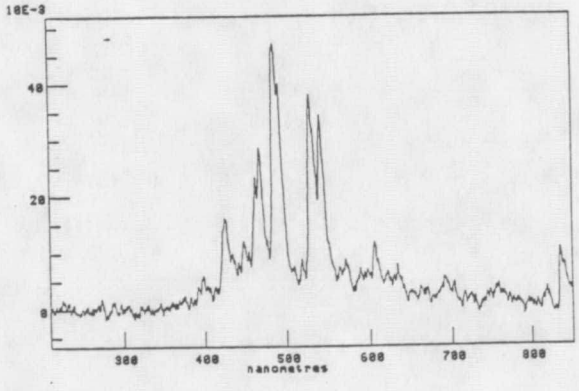

Figure 7. Beam Spectrum at V_B = 1,100 V; I_D = 500 mA

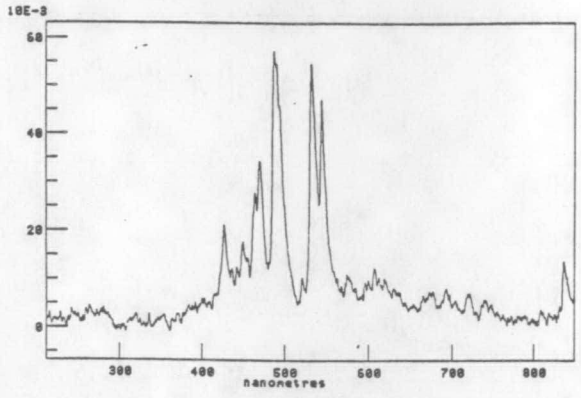

Figure 8. Beam Spectrum at V_B = 1,300 V;
I_D = 500 mA

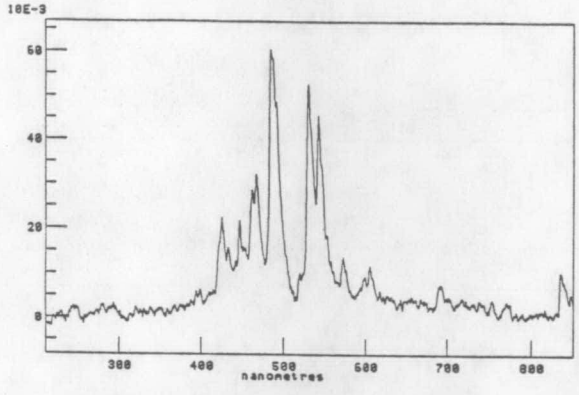

Figure 9. Beam Spectrum at V_B = 1,500 V;
I_D = 500 mA

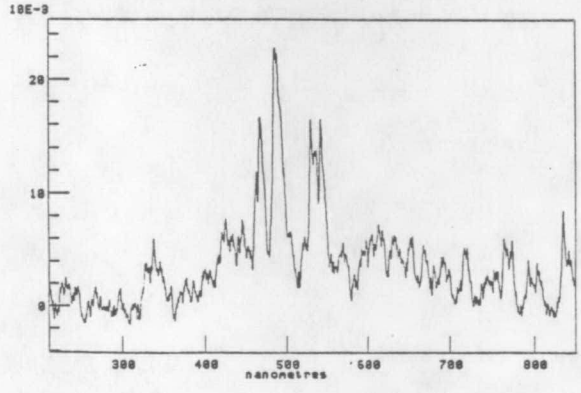

Figure 10. Beam Spectrum at V_B = 1,100 V;
I_D = 250 mA

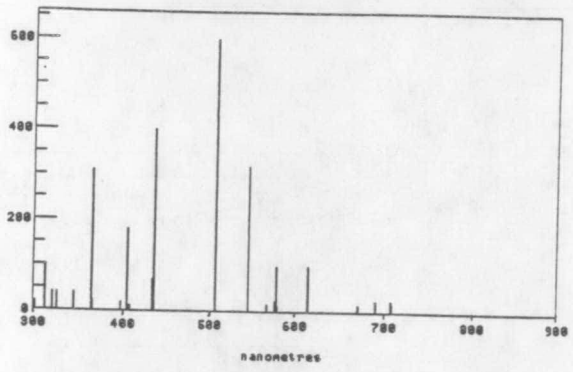

Figure 11. Computer Generated Histogram of the Mercury Spectrum

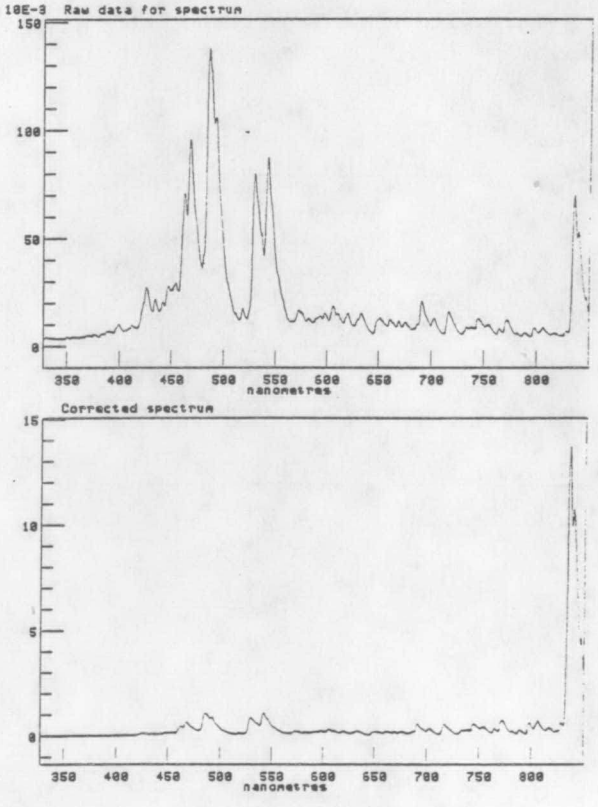

Figure 12. Discharge Spectrum at 5.0 A Discharge Current

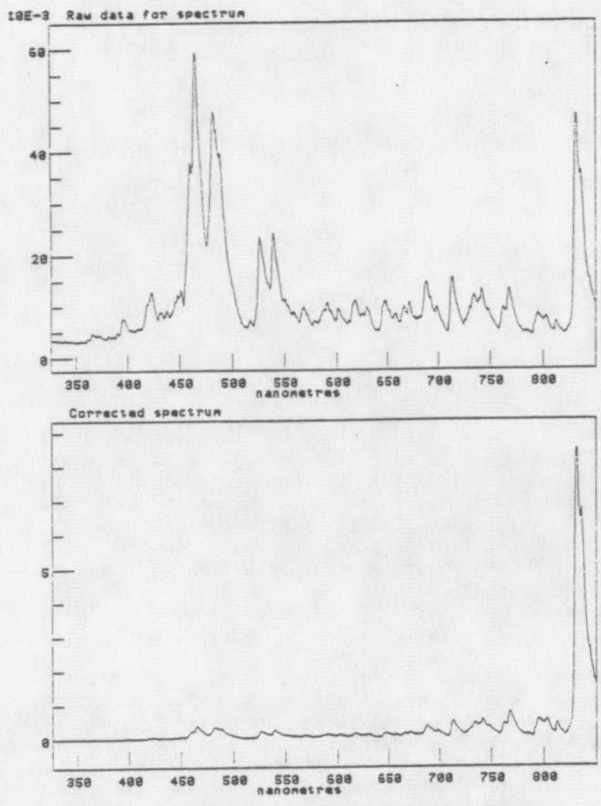

Figure 13. Discharge Spectrum at 2.5 A Discharge Current

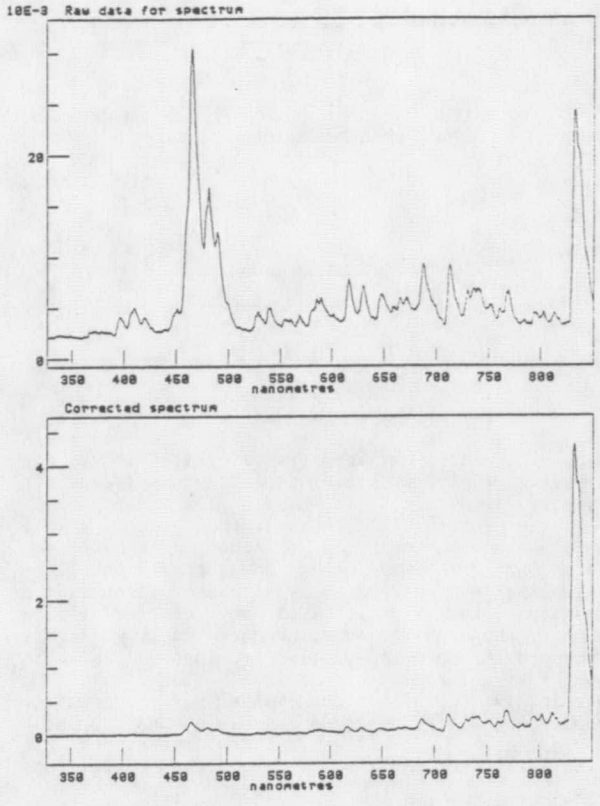

Figure 14. Discharge Spectrum at 1.0 A Discharge Current